Simulation of The Pharmacokinetic Profile of Methazolamide in Blood: Effect of Erythrocyte Carbonic Anhydrase Binding on Drug Disposition

Malaz A. AbuTarif[1] and David R. Taft[1,2]

Received October 8, 2001; accepted January 4, 2002

KEY WORDS: methazolamide; pharmacokinetics; disposition; simulation; protein binding; distribution.

INTRODUCTION

The erythrocytes play an important, yet oftentimes ignored, role in the transport and disposition kinetics of medications in the blood (1,2). For those compounds that accumulate in erythrocytes to an appreciable extent, significant pharmacokinetic information can be obtained through characterization of the different kinetic events occurring within the erythrocyte.

Methazolamide (MTZ) is a carbonic anhydrase inhibitor (CAI) that is used for the management of glaucoma (3). MTZ is a methylated tautomer of acetazolamide, the most widely studied CAI (4). Carbonic anhydrase (CA) is a family of enzymes that catalyze the reversible hydration of carbon dioxide. Seven isozymes (denoted CA-I through CA-VII) have been identified in humans, each varying in activity and tissue distribution (5,6). In humans, greater than 90% of total CA enzyme resides in the erythrocytes, where there are two isozymes present: CA-I and CA-II. CA-I, a polymer composed of a single promoter, has a low affinity and high capacity. In contrast, CA-II contains two promoters and is a high-affinity, low-capacity isozyme (7).

Several investigators have studied the *in vivo* disposition of MTZ. Bayne *et al.* (8) reported a half-life of 15 days for MTZ in red blood cells (RBCs). In contrast, the plasma half-life was reported to be only 14–20 h (9). This discrepancy between plasma and RBC data has been attributed to the differential binding of MTZ to CA-I and CA-II in the erythrocyte (10,11).

A recent investigation by Iyer *et al.* (12) characterized the erythrocyte distribution of MTZ i*n vitro*. A model was developed to describe MTZ erythrocyte transport and binding kinetics with CA isozymes (12). By describing the non-instantaneous erythrocyte distribution of MTZ, this model may be able to predict MTZ disposition *in vivo*.

In this present study, the influence of the kinetics of drug binding to CA isozymes I and II on the pharmacokinetic profile of MTZ *in vivo* was investigated using computer simulations for single and multiple oral dosing regimens. The objective of this study was to explain the discrepancies among the published pharmacokinetic parameters of MTZ and to describe the temporal disposition of MTZ in blood and plasma. A physical model was developed that described MTZ absorption, distribution, and elimination *in vivo*. The resulting values for MTZ pharmacokinetic parameters were compared to those previously published in the literature.

[1] Division of Pharmaceutics and Industrial Pharmacy, Long Island University, 1 University Plaza, Brooklyn, New York 11201.

[2] To whom correspondence should be addressed. (e-mail: dtaft@liu.edu)

EXPERIMENTAL

Theoretical Model

A schematic representation of the model used in this study is provided in Figure 1. The absorption of MTZ was assumed to follow simple diffusion described by a first-order process with no lag time. This assumption was based on previous published studies (11). Subsequently, the rate of disappearance of MTZ from the gastrointestinal tract (X_G) can be described using the following equation:

$$\frac{dX_G}{dt} = -k_a \cdot X_G \tag{1}$$

where k_a represents the first-order absorption rate constant. Assuming 80% bioavailability, the administered dose is the initial condition for Eq. 1.

MTZ erythrocyte permeation was also described according to Fick's law (13). Therefore, the rate of change of MTZ plasma concentrations can be expressed as follows:

$$\frac{dC_p}{dt} = \frac{k_a \cdot X_G}{V_p} - P' \cdot (C_p \cdot f_p - C_{RBC,f}) - k_e \cdot C_p \tag{2}$$

The driving force for erythrocyte permeation is the concentration gradient of free drug between plasma and the RBCs. f_p in Eq. 2 is the plasma-free fraction of MTZ and $C_{RBC,f}$ represents the free RBC concentration. P' is defined as the permeability rate constant and equals erythrocyte membrane permeability of MTZ multiplied by the surface area and divided by the volume (AP/V, reference 13). V_p and k_e represent the plasma volume (3 liter) and first-order elimination rate constant for MTZ, respectively. Distribution to tissues other than RBCs was assumed to be negligible. This assumption was derived from published clinical data (8,10,11). It is implied in the model that plasma protein binding is non-saturable (i.e., f_p is constant) over the range of plasma concentrations studied. The validity of this assumption was previously established in the laboratory (11).

$C_{RBC,f}$ can be described using the following rate equation:

$$\frac{dC_{RBC,f}}{dt} = P' \cdot (C_p \cdot f_p - C_{RBC,f}) - k_1 \cdot C_{RBC,f} \cdot E_1 + k_{-1} \cdot EC_1 - k_2 \cdot C_{RBC,f} \cdot E_2 + k_{-2} \cdot EC_2 \tag{3}$$

where E_1 and E_2 are the concentrations of free isozymes I and II, respectively. EC_1 and EC_2 are the concentrations of bound isozymes. Total enzyme concentrations (ET_1 and ET_2) are assumed to be the sum of free and drug bound enzyme concentrations:

$$ET_1 = E_1 + EC_1; \tag{4}$$

0724-8741/02/0400-0551/0 © 2002 Plenum Publishing Corporation

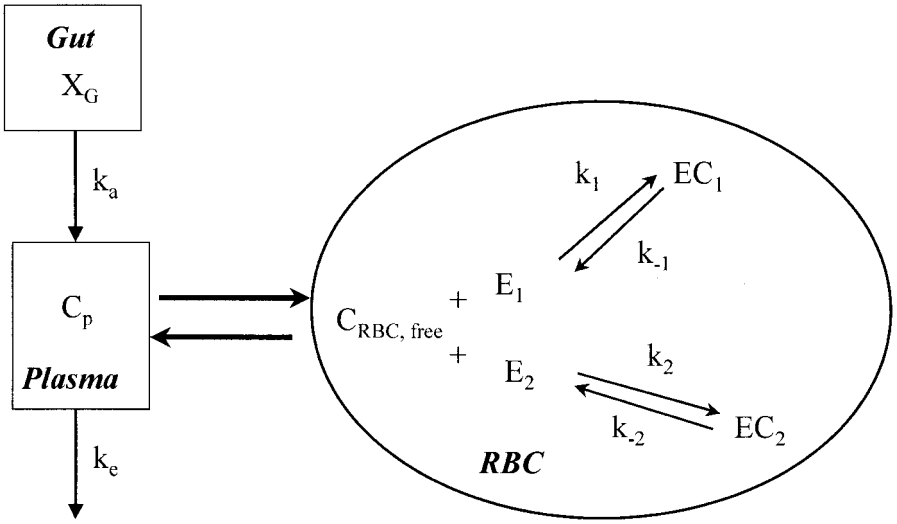

Fig. 1. Schematic representation of proposed model for MTZ disposition *in vivo*.

$$ET_2 = E_2 + EC_2 \quad (5)$$

Substituting Eqs. 4 and 5 into Eq. 3, the following relationship is obtained:

$$\frac{dC_{RBC,f}}{dt} = P'(\cdot)(C_p \cdot f_p - C_{RBC,f}) - k_1 \cdot C_{RBC,f} \cdot (ET_1 - E_1) + k_{-1} \cdot EC_1 - k_2 \cdot C_{RBC,f} \cdot (ET_2 - EC_2) + k_{-2} \cdot EC_2 \quad (6)$$

The binding kinetics between MTZ and CA-I and CA-II can be described using the following two differential equations:

$$\frac{d(EC_1)}{dt} = k_1 \cdot C_{RBC,f} \cdot (ET_1 - EC_1) - k_{-1} \cdot EC_1 \quad (7)$$

$$\frac{d(EC_2)}{dt} = k_2 \cdot C_{RBC,f} \cdot (ET_2 - EC_2) - k_{-2} \cdot EC_2 \quad (8)$$

The model described above represents an attempt to explain the physical nature of MTZ pharmacokinetics. A similar model was previously used to characterize MTZ erythrocyte distribution *in vitro* (12).

Model Simulation: Single-Dose Administration

The differential Eqs. 1, 2, 6, 7, and 8 were numerically solved using MathCad 7.0 version (MathSoft, Inc.). The Rkadapt command was used. This command employs Runge–Kutta algorithm with adaptive intermediate steps (fifth order). Rkadapt uses nonuniform (variable) step sizes internally when it solves differential equations, but returns the solution at equally spaced points.

Values for model parameters are listed in Table I. The rate constants for the binding kinetics to the isozymes (k_1, k_2, k_{-1}, and k_{-2}) were obtained from an *in vitro* study of MTZ erythrocyte distribution (12). The estimate of k_e was obtained from the literature (11). The value for f_p (0.4) was within range of reported values (0.28–0.45, references 8 and 11). Manual iterations of model equations were performed to obtain parameter estimates for k_a such that the resultant plasma t_{max} was consistent with published data. Likewise, values for P', ET_1, and ET_2 were optimized to produce clinically relevant blood:plasma concentration ratios. Simulations were then performed using a range of oral doses (25, 50, 75, 100, and 150 mg) for two time intervals post-dose: 48 h and 7200 h.

Table I. Values for Parameters Used in Model Simulations[a]

Parameter	Description	Estimate
k_a[b]	First-order absorption rate constant	0.2 h^{-1}
V_p	Volume of plasma compartment	3000 mL
f_p[c]	Fraction unbound in plasma	0.4
k_e[d]	First-order rate constant describing other disposition processes	0.035 h^{-1}
P'	Permeability rate constant	5 h^{-1}
k_2[e]	Rate constant describing drug binding to high affinity CA-II (forward reaction)	186 mL/μg · h
k_1[e]	Rate constant describing drug binding to low affinity CA-I (forward reaction)	0.132 mL/μg · h
ET_2[b]	Maximum binding capacity for CA-II	50 μg/mL
ET_1[b]	Maximum binding capacity for CA-I	200 μg/mL
k_{-2}[e]	Rate constant describing drug binding to high affinity CA-II (reverse reaction)	95.4 h^{-1}
k_{-1}[e]	Rate constant describing drug binding to low affinity CA-I (reverse reaction)	15.2 h^{-1}

[a] Please refer to Figure 1 for schematic overview of the model.
[b] Parameter estimate optimized to produce clinical relevant concentrations in plasma and blood.
[c] Estimate within range of reported values (0.28–0.45, References 10 and 11).
[d] Estimate obtained from Reference 11.
[e] Estimate obtained from Reference 12.

Whole blood concentrations were calculated using the following equation:

$$C_{Blood} = C_{RBC} \cdot Hct + C_p \cdot (1 - Hct) \quad (9)$$

where Hct represents the hematocrit. An Hct value of 0.5 was used in this study. RBC concentrations were calculated by adding simulated values of $C_{RBC,f}$ and concentrations of MTZ bound to both E_1 and E_2 (EC_1 and EC_2).

Model Simulation: Multiple-Dose Administration

Multiple-dose simulations were also conducted using MathCad 7.0. A dosing regimen of 100 mg daily was simulated and concentrations were plotted against their prospective time points. Simulations were performed for single dose administration (i.e., the first administered dose) as described above. At the times for administration of successive doses, the simulation was repeated using concentrations from the end of the previous simulation period as the initial conditions for model equations.

RESULTS AND DISCUSSION

Single-dose simulations were performed for oral doses ranging from 25 to 150 mg. Figure 2 illustrates the model-predicted disposition of MTZ after oral administration of a 100-mg dose. Data were analyzed for 48 h post-dose. As seen in the figure, the model-predicted t_{max} values for RBC, blood, and plasma were 25, 24.5, and 1.5 h, respectively. The results

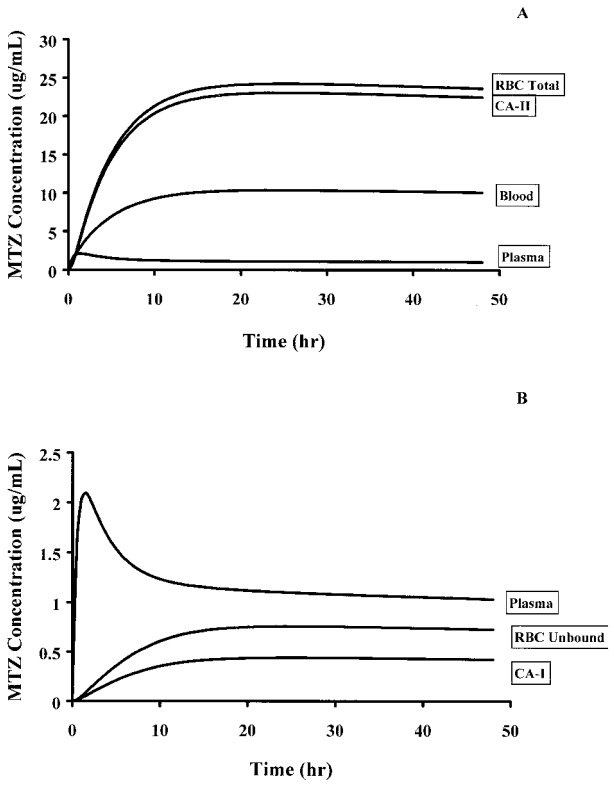

Fig. 2. Model simulated concentrations vs. time after single-dose oral administration of MTZ (100 mg). Simulations were performed for 48 h post-dose. (A) Total RBC, CA-II bound, blood and plasma concentrations. (B) Plasma, unbound RBC, and CA-I bound concentrations.

demonstrate that distributional equilibrium between plasma and RBCs was not reached 48 h after single-dose administration of MTZ. Similar differences in t_{max} have been observed clinically (8,10). Previous *in vitro* studies have established that RBC penetration of MTZ is a relatively rapid process (13). Therefore, the delayed distribution of MTZ cannot be explained by permeability rate-limited erythrocyte uptake of MTZ. As demonstrated by the model, these observations can be attributed to kinetics of MTZ binding to CA isozymes present in the erythrocyte (CA-I and CA-II).

Table II presents the model-predicted peak concentrations of MTZ in RBCs, plasma, and whole blood after single-dose oral administration of MTZ (range 25–150 mg). Comparison of plasma and RBC data indicates a high apparent partitioning of MTZ in erythrocytes. The linearity of simulated RBC concentrations with increasing dose implies that erythrocyte binding of MTZ was not saturated by doses as high as 150 mg.

Included in Table II are data previously published by Pradhan *et al.* (10). Over the dosing range tested, simulated data for blood and RBCs were consistent with those observed clinically. However, at low doses of MTZ (25 and 50 mg), model-predicted plasma concentrations were significantly greater than the reported values. The apparent nonlinear behavior of plasma data with increasing dose (reported data, Table II) was attributed to the differential binding between MTZ and CA-I and CA-II; that is, MTZ binds primarily to CA-II (the high-affinity isozyme) at low doses (25–50 mg), resulting in very low plasma concentrations (10). At higher doses, CA-II becomes saturated and MTZ binds primarily to CA-I. Because this is a low affinity isozyme, plasma concentrations rise disproportionately with dose.

As demonstrated in Table II, peak plasma concentrations simulated by the model increased linearly with dose. Therefore, differential binding between MTZ and the two CA isozymes in the erythrocytes cannot explain the reported nonlinear behavior of MTZ in plasma after single doses (10). An alternative explanation to account for the apparent nonlinear behavior of MTZ in plasma observed clinically is extravascular tissue distribution. Because CA enzymes are pre-

Table II. Model-Simulated Peak MTZ Concentrations in Plasma, Whole Blood, and Erythrocytes: Comparison to Reported Data[a]

Matrix	Dose (mg)	Model-simulated C_{max} (μg/mL)[b]	Reported C_{max} (μg/mL)[c]
Plasma	25	0.47	0.1 ± 0.1
	50	1.05	0.2 ± 0.1
	100	2.1	1.5 ± 1.5
	150	3.2	Not reported
Blood	25	3.1	2.8 ± 0.8
	50	5.9	6.3 ± 2.4
	100	10.4	14.3 ± 4.3
	150	15.5	Not reported
Erythrocytes	25	6.1	6.4 ± 2.2
	50	12.3	13.7 ± 5.4
	100	24.2	31.2 ± 10.1
	150	35.2	Not reported

[a] Data obtained from Reference 10.
[b] Concentrations predicted through simulation of proposed model of MTZ disposition.
[c] Data reported as mean ± SD from 5–6 subjects.

dominantly found in erythrocytes (greater than 90%), the model assumed negligible distribution to tissues other than RBCs. However, CA enzymes (specifically the high affinity type, CA-II) are present in other organs of the body (kidney, brain, and lungs). Distribution to these sites might influence the plasma concentrations after single dose administration of low doses (25 and 50 mg), the effect becoming less significant when a higher dose is given.

In addition to the 48-h simulation exercise, model simulations were performed over an extended time period post-dose: 300 days. The results are presented in Figure 3, a plot of MTZ disposition following oral administration (100 mg). As illustrated in the Figure 3C, MTZ was present in RBCs for more than 1000 h. The results are consistent with a previous study by Bayne *et al.* (8), who measured MTZ (equivalent to ≈ 6% total dose) in RBCs 45 days after drug administration (150 mg). These findings demonstrate that the developed model of CA binding kinetics can explain the prolonged residence of MTZ *in vivo*.

The results of multiple dosing simulations are provided in Figure 4A, a plot of peak concentrations (plasma, RBC, blood) as a function of the number of doses (100 mg) administered. In contrast to the single-dose simulations (Table II), where dose-linearity was demonstrated, there is evidence that

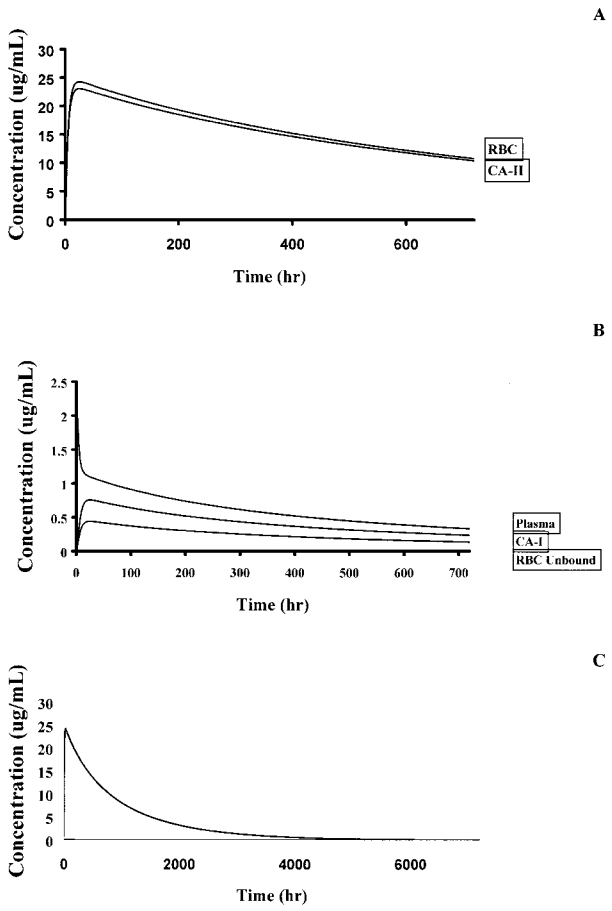

Fig. 3. Model-simulated concentrations vs. time after single-dose oral administration of MTZ (100 mg). (A) Total RBC and CA-II bound concentrations for 700 h. (B) Plasma, unbound RBC, and CA-I-bound concentrations for 700 h. (C) RBC-simulated concentrations for 7200 h post-dose.

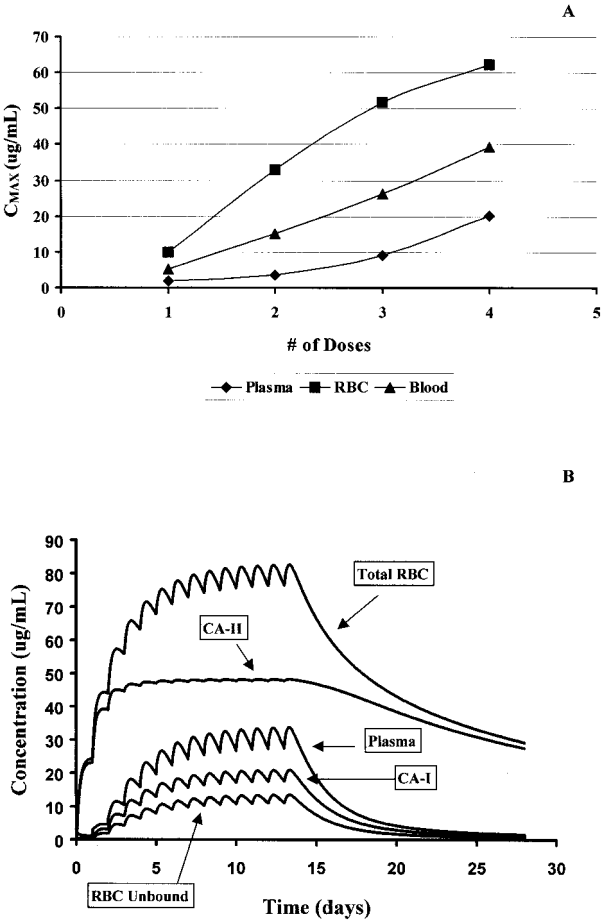

Fig. 4. (A) Dose proportionality of MTZ in plasma, RBCs, and blood after multiple-dose administration (100 mg every 24 h). Data are presented as predicted maximum concentrations vs. number of of doses administered. (B) Model-simulated concentrations vs. time after multiple-dose oral administration of MTZ (100 mg every 24 h).

RBC binding approaches saturation after multiple-dose administration. Given the apparently long elimination half-life of MTZ, significant accumulation would be expected with daily dosing. As seen in Figure 4B, RBC concentrations begin to reach a plateau with repeated dose administration. Conversely, plasma concentrations increase disproportionately with dose, secondary to RBC saturation. This dramatic rise in plasma concentrations is likely to predispose the patient to a greater risk of adverse drug reactions. The development of side effects was recently reported in patients receiving daily doses of MTZ (75 to 100 mg) for 2 weeks (14).

The predominant form of carbonic anhydrase in the erythrocyte is CA-I, a low affinity isozyme. However, single-dose simulations (100-mg dose, depicted in Fig. 2) indicate that MTZ is bound primarily to CA-II, the high affinity isozyme. Consequently, the terminal phase of the concentration time plot (i.e., the elimination half-life) is controlled by the release kinetics from CA-II. Being a low capacity enzyme, CA-II would be expected to saturate with multiple-dose administration of MTZ (or administration of a large single dose). As illustrated in Figure 4, CA-II approaches saturation after several doses. Subsequently, MTZ complexation with CA-I increases dramatically with successive administration of MTZ. When the dosing regimen depicted in the figure is ter-

minated, a biphasic decay of RBC concentration is observed. The relatively rapid decline in erythrocyte concentrations (i.e., 50% decline between days 15–20 in Fig. 4B) is a result of drug release from the low affinity isozyme CA-I. CA-I will readily give up MTZ in response to drug clearance from the plasma, thereby maintaining equilibrium. As total RBC levels approach those of CA-II, a much slower elimination rate is observed at later time points (25+ days, Fig. 4B). Although this biphasic elimination pattern was not observed with the single-dose simulations (because CA-II levels were below saturation, Fig. 3), this phenomenon has been observed clinically (8,10).

Another interesting aspect of MTZ disposition is the observation that RBC concentrations approach steady state faster than plasma concentrations (8). Based on linear pharmacokinetics, five half-lives are required to reach steady state. Because MTZ has a longer apparent half-life in RBCs compared to plasma, steady state would predictably be attained in plasma before RBCs. As seen in Figure 4, however, RBC concentrations approach steady state earlier than plasma levels. This discrepancy can again be attributed to the binding kinetics of MTZ to the high affinity isozyme (CA-II). A binding affinity constant (K_{aff}) is simply the ratio of rate constants describing forward (denoted as k_2 for CA-II in the model) and reverse binding reactions (k_{-2}), respectively. A high-affinity constant infers that $k_2 >> k_{-2}$. Steady state is achieved earlier in RBCs because of the strong attraction of MTZ to CA-II, reflected in a strong forward binding reaction. Conversely, the long half-life in RBCs is due to small value of k_{-2} and a slow dissociation of MTZ from the isozyme.

It is clear from the results presented in this work that protein-binding kinetics may significantly influence the pharmacokinetics of a compound. The assumption that drug binding to enzymes and proteins happens relatively fast (in often cases assumed to occur instantaneously) compared to other disposition processes may not always be valid. In the case of MTZ, the information gleaned from *in vitro* experiments provided valuable insight correlating the kinetics of enzyme binding with elimination *in vivo.* Moreover, this type of approach potentially may be applied to other situations where the pharmacokinetic disposition of a medication is governed by tissue distribution processes. This would allow for development of more efficacious dosing regimens or improving the safety margins of these compounds.

Computer simulations using pharmacokinetic models can be a useful tool to help with clinical decision-making and therefore to improve the drug discovery and development process. However, the selection and/or development of an appropriate model are a critical step in this process as simpler models are not always satisfactory. As demonstrated in this study, data obtained from preclinical pharmacokinetic experiments can be used to successfully predict drug disposition in the clinical setting. It should be noted, however, that further studies are needed to establish the validity of the model and model parameters utilized in this research.

REFERENCES

1. M. S. Highley and E. A. DeBruijin. Erythrocytes and the transport of drugs and endogenous compounds. *Pharm. Res.* **13**:186–195 (1996).
2. P. H. Hinderling. Red blood cells: a neglected compartment in pharmacokinetics and Pharmacodynamics. *Pharmacol. Ref.* **49**: 279–295 (1997).
3. P. J. Wistrand. The use of carbonic anhydrase inhibitors in ophthalmology and medicine. *Ann. NY Acad. Sci.* **429**:609–619 (1984).
4. C. T. Supuran, F. Brigant, and A. Scozzafava. Sulfonamidosulfonamides as inhibitors of carbonic anhydrase isozymes I, II, and IV. *J. Enzyme Inhib.* **12**:175–190 (1997).
5. S. Lindskog and P. Nyman. Metal binding properties of human erythrocyte carbonic anhydrase. *Biochim. Biophys. Acta* **86**:462–474 (1964).
6. S. Lindskog, L. E. Henderson, and K. K. Kannan. *Carbonic Anhydrase: The Enzymes, 3ed edition*, Academic Press, New York, 1971.
7. P. J. Wistrand and P. Baathe. Inhibition of carbonic anhydrase activity of whole erythrocytes. *Acta Pharmacol. Toxicol.* **26**:145–168 (1968).
8. W. F. Bayne, F. T. Tao, G. Rogers, L. C. Chu, and F. Fheeuwes. Time course and disposition of methazolamide in human plasma and red blood cells. *J. Pharm. Sci.* **70**:75–81 (1981).
9. T. H. Maren, J. R. Haywood, S. K. Chapman, and T. J. Zimmerman. The pharmacology of methazolamide in relation to the treatment of glaucoma. *Invest. Ophthalmol. Vis. Sci.* **16**:730–742 (1977).
10. S. Pradhan, S. Praohan, A. T. Wu, L. L. Lesko, M.-L. Chen, and R. L. Williams. Bioavailability measurements of methazolamide in plasma, red blood cells and whole blood: Implications for bioequivalence studies. *Int. J. Pharm.* **138**:207–213 (1996).
11. D. R. Taft, S. Nordt, G. R. Iyer, and M. H. Schwenk. Blood disposition and urinary excretion kinetics of methazolamide following oral administration to human subjects. *Biopharm. Drug Dispos.* **19**:373–380 (1998).
12. G. R. Iyer, R. A. Bellantone, and D. R. Taft. *In vitro* characterization of the erythrocyte distribution of methazolamide: a model of erythrocyte transport and binding kinetics. *J. Pharmacokinet. Biopharm.* **27**:45–66 (1999).
13. L. B. Holder and S. L. Hayes. Diffusion of sulfonamides in aqueous buffers and into red cells. *Mol. Pharmacol.* **1**:266–279 (1965).
14. S. Shirato, F. Kagaya, Y. Suzuki, and S. Joukou. Stevens-Johnson syndrome induced by methazolamide treatment. *Arch. Ophthalmol.* **4**:550–553 (1997).